arXiv:hep-ph/9610282v1 8 Oct 1996

IM SB RAS NNA 6-96

The interference in the reaction $e^+e^- \to \gamma\pi^+\pi^-$ and the search for the decay $\phi \to \gamma f_0 \to \gamma\pi^+\pi^-$. [*]

N.N. Achasov, V.V. Gubin and E.P. Solodov [†]

Laboratory of Theoretical Physics

S.L. Sobolev Institute for Mathematics

Novosibirsk-90, 630090, Russia [‡]

(February 1, 2008)

Abstract

We describe the interference between amplitudes $e^+e^- \to \rho \to \gamma\pi^+\pi^-$ and $e^+e^- \to \phi \to \gamma f_0 \to \gamma\pi^+\pi^-$, where f_0 meson is considered in the frameworks of the four-quark model and the model of the scalar $K\bar{K}$ molecule. The general expressions for the differential cross section with the radiative corrections and two angle cuts are given. The interference patterns are obtained in the spectrum of the differential cross section by the energy of the photon and in the full cross section by the energy of the beams.

12.39.-x, 13.40.Hq.

Typeset using REVTEX

---

[*] This work was partly supported by Russian Fund for Basic Research , grants 94-02-05 188, 96-02-00 548 and by INTAS-94-3986

[†] The Budker Institute for Nuclear Physics , Novosibirsk-90, 630090, Russia

[‡] E-mail: achasov@math.nsc.ru

A. Introduction.

The elucidation of puzzle of scalar f_0 and a_0 mesons has became the central problem of light hadron spectroscopy. As it is known the properties of the scalar f_0 and a_0 mesons are mysterious from the naive quark model point of view. The long study of these mesons [1–3] has shown that all challenging properties of the f_0 and a_0 mesons can be described naturally in the framework of the four-quark ($q^2\bar{q}^2$) MIT-bag model [4]. Along with it the other possibilities are discussed in the literature [5–8]: the model of scalar $K\bar{K}$ molecules, glueballs and so on. This model variety has risen up the question of looking for the processes permitting to choose the most adequate one from all abundance. During years of time there was established by efforts of theorists that the study of the radiative decays $\phi \to \gamma f_0 \to \gamma\pi\pi$ and $\phi \to \gamma a_0 \to \gamma\pi\eta$ could play a crucial role in the elucidation of the nature of the scalar f_0 and a_0 mesons [9–12].

At present time the investigation of the $\phi \to \gamma f_0 \to \gamma\pi^+\pi^-$ decay has started with the detector CMD-2 [13] at the e^+e^--collider VEPP-2M in Novosibirsk. Besides that, in Novosibirsk at the same collider the detector SND has put into operation [14] and now it has been working with $e^+e^- \to \gamma f_0 \to \gamma\pi^0\pi^0$ and $e^+e^- \to \gamma a_0 \to \gamma\eta\pi^0$ decays. The modernization of the VEPP-2M complex has been planed aiming to increase the luminosity to one order of magnitude. And, finally, in the nearest future in Frascati the start of the operation of the ϕ-factory DAΦNE is expected, which, probably, makes possible studying the scalar $f_0(980)$ and $a_0(980)$ mesons in exhaustive way.

Experimentally the radiative decays $\phi \to \gamma f_0 \to \gamma\pi\pi$ are studied observing the interference patterns in the reaction $e^+e^- \to \gamma\pi\pi$ at the ϕ meson peak. Analysis of interference patterns in these reactions, especially in the charged channel $e^+e^- \to \gamma\pi^+\pi^-$, is the rather difficult problem to which a great attention was paid in the literature [15–17]. But the careful examination of the literature has shown that the analysis of interference patterns in the reaction $e^+e^- \to \gamma\pi^+\pi^-$ was not only carried out in exhuastive way but also was improper either from the theoretical point of view or from the experimental one. In particular, the intermediate $K\bar{K}$ states, at the thresholds of which the scalar resonances lie, was not taken into account in the propagators. In papers [15–17] also there was not taken into account the fact that the narrow width approximation is not valid in considered case [18], so that all branching ratios of the radiative decays of the ϕ meson into the scalar a_0 and f_0 mesons are at least two times overstated, see [18]. The formulae given in [15–17] do not take into account the radiative corrections that are quite important, see below.

Besides that, all aforementioned papers have studied the interference pattern in the photon spectrum meanwhile the interference pattern in the full cross section not only complements that one but could be much more important in some particular cases, at low statistics for example.

In this paper we give the full analysis of interference patterns in the reaction $e^+e^- \to \gamma\pi^+\pi^-$ at the ϕ meson peak considering two models: the four-quark ($q^2\bar{q}^2$) model and the model of the scalar $K\bar{K}$ molecule. We take our cues from the preliminary data obtained in the experiment [13].

The paper is organized in the following way.

In the section II we consider the reaction $e^+e^- \to \gamma\pi^+\pi^-$ and give the necessary formulae for this process with taking into account the cuts of the angle between the photon momentum and electron beam and of the angle between the photon and π^+ meson momenta in the dipion rest frame. We consider the radiative corrections to the full cross section of the process in that section as well. The propagators and model depending quantities are described in the section III. The section IV is devoted to the interference pattern in the spectrum of the photon energy at the ϕ meson peak and the interference pattern in the full cross section by the total energy of the beams at the ϕ meson region. In the conclusion we discuss the possibility of experimental investigation of interference patterns in the reaction $e^+e^- \to \gamma\pi^+\pi^-$. The appendix gives the expressions for the cross section of the $e^+e^- \to \gamma\mu^+\mu^-$ process which is the background for the $e^+e^- \to \gamma\pi^+\pi^-$ reaction and gives the values for $BR(\phi \to \gamma^* \to \rho \to \gamma\pi^+\pi^-)$ and $BR(\phi \to \gamma^* \to \gamma\mu^+\mu^-)$ as well.

I. AMPLITUDES $e^+e^-\to\phi\to\gamma f_0\to\gamma\pi^+\pi^-$ AND $e^+e^-\to\rho\to\gamma\pi^+\pi^-$.

We consider the production of the f_0 meson through the loop of the charged K mesons, $\phi\to K^+K^-\to\gamma f_0$, see [9,10]. Diagram is presented in Fig. 1a. The production amplitude $\phi\to\gamma f_0$ in the rest frame of the ϕ meson is:

$$M = g_R(t)\vec{e}(\phi)\vec{e}(\gamma) \tag{1}$$

where $t=(k_+ + k_-)^2$, $\vec{e}(\phi)$ and $\vec{e}(\gamma)$ are the polarization vectors of the ϕ meson and the photon respectively. The expressions for $g_R(t)$ are obtained in the four-quark ($q^2\bar{q}^2$) model [9] and in the scalar $K\bar{K}$ molecule model [12]. Note, that in the four-quark model the scalar mesons are considered as a point like objects and in the scalar $K\bar{K}$ molecule model as extended ones [5].

The amplitude of the reaction $e^+e^-\to\phi\to\gamma f_0\to\gamma\pi^+\pi^-$ is

$$M = e\bar{u}\gamma^\mu u\frac{em_\phi^2}{f_\phi}\frac{g_{f_0\pi\pi}}{sD_\phi(s)D_{f_0}(t)}g_R(t)(q^\mu\frac{e(\gamma)p}{pq} - e(\gamma)^\mu) \tag{2}$$

where $s=p^2=(p_1+p_2)^2$, and $g_R(t)\sim(s-t)\sim(pq)\to 0$ at $(pq)\to 0 \quad (t\to s)$. The coupling constants $g_{f_0\pi\pi}$ and f_ϕ are related to the widths in the following way: [1]

$$\Gamma(f_0\to\pi\pi,t) = \frac{g^2_{f_0\pi\pi}\sqrt{t-4m_\pi^2}}{16\pi t}, \qquad \Gamma(V\to e^+e^-,s) = \frac{4\pi\alpha^2}{3}(\frac{m_V^2}{f_V})^2\frac{1}{s\sqrt{s}}. \tag{3}$$

The width of the ϕ meson decay is

$$\Gamma(\phi\to\gamma f_0\to\gamma\pi^+\pi^-) = \frac{1}{\pi}\int_{4m_\pi^2}^{m_\phi^2}\sqrt{t}dt\frac{\Gamma(f_0\to\pi^+\pi^-,t)\Gamma(\phi\to\gamma f_0,t)}{|D_{f_0}(t)|^2}, \tag{4}$$

where

$$\Gamma(\phi\to\gamma f_0,t) = \frac{1}{3}\frac{|g_R(t)|^2}{4\pi}\frac{1}{2m_\phi}(1-\frac{t}{m_\phi^2}). \tag{5}$$

The propagators of the ϕ and f_0 mesons $D_\phi(s)$ and $D_{f_0}(t)$ will be described below.

---

[1] $\Gamma(f_0\to\pi^+\pi^-,t) = \frac{2}{3}\Gamma(f_0\to\pi\pi,t)$

For the differential cross section we get the expression:

$$\frac{d\sigma_\phi(e^+e^-\to\gamma f_0\to\gamma\pi^+\pi^-)}{dt d\cos\theta_\gamma}=\frac{1}{\pi}\frac{\sqrt{t}\Gamma(f_0\to\pi^+\pi^-,t)\frac{d\sigma}{d\cos\theta_\gamma}(e^+e^-\to\gamma f_0,t)}{|D_{f_0}(t)|^2}. \tag{6}$$

Having done the integration over angle θ_γ we get

$$\frac{d\sigma_\phi}{d\omega}=\frac{\alpha^2}{24\pi s^2\sqrt{s}}\left(\frac{g_{f_0\pi\pi}}{f_\phi}\right)^2\frac{m_\phi^4}{|D_\phi(s)|^2}\frac{|g_R(t)|^2}{|D_{f_0}(t)|^2}(s-t)\sqrt{1-\frac{\xi}{1-x}}\quad(a+\frac{a^3}{3})b \tag{7}$$

where $\omega=|\vec{q}|$ is the energy of the photon. Following [15,17] we identify $\xi=\frac{4m_\pi^2}{s}$ and $x=\frac{2\omega}{\sqrt{s}}$, $t=s(1-x)$. We also introduce two symmetrical angle cuts: $-a\le\cos\theta_\gamma\le a$, where θ_γ is the angle between the photon momentum and the electron beam in the center of mass frame of the reaction under consideration and $-b\le\cos\theta_{\pi\gamma}\le b$, where $\theta_{\pi\gamma}$ is the angle between the photon and the π^+ meson momenta in the dipion rest frame.

As it was shown in the previous papers [15,16] the basic background to the process under study has came from the initial electron radiation (see Fig.1d) and the radiation from the final pions (Fig.1c). The initial state radiation does not interfere with the final state radiation and with the signal in the differential cross section integrated over all angles since the charged pions are in the C=-1 state. This is true also when the angle cuts are symmetrical.

Introducing the symmetrical angle cuts considerably decreases the background from the initial state radiation because of the photons in this case are emitted along the beams mainly. The restriction on the energy of photons $20<\omega<100\ MeV$ cuts the background from the radiative process with the radiation of hard photons.

In our region $20<\omega<100\ MeV$ the background from the nonresonant by invariant mass of $\pi^+\pi^-$ system processes, see Fig.1e, is negligible. Its contribution to $BR(\phi\to\gamma\pi^+\pi^-,20<\omega<100\ MeV)<2,2\cdot10^{-7}$ and therefore we do not take into account it.

Let us consider the background related to the final state radiation. The amplitude of the process is

$$M_\rho=e^2\bar{u}\gamma^\mu u\frac{em_\rho^2}{f_\rho}\frac{1}{sD_\rho(s)}2g_{\rho\pi\pi}T^\mu, \tag{8}$$

$$T^\mu=\frac{e(\gamma)k_-}{qk_-}(k_+-\frac{p}{2})^\mu+\frac{e(\gamma)k_+}{qk_+}(k_--\frac{p}{2})^\mu+e(\gamma)^\mu$$

It is necessary to take into account the contribution of the $\phi-\rho$ transition when studying the interference pattern in the full cross section, see Fig.1c, the quantity which modulus is as great as 15% in comparison with the modulus of the main term.

Taking into account the vacuum polarization we get

$$M = M_\rho\left(1 - Z\frac{m_\phi \Gamma_\phi}{D_\phi(s)}\right) = M_\rho\left(1 - \frac{3\Gamma(\phi \to e^+e^-)\sqrt{s}}{\alpha D_\phi(s)}\right). \tag{9}$$

For simplicity sake, we restricted our expression only to the photon contribution which is the main in the $\phi - \rho$ transition, see Fig.1f. Note, that the diagram of Fig.1b is not significant since it is proportional to $1/D_\rho$ and is negligible in the ϕ meson peak.

It is convenient to give the differential cross section in the form:

$$\begin{aligned}
&\frac{d\sigma_f}{d\omega} = 2\sigma_0(s)\frac{1}{\sqrt{s}}F(x,a,b)\left|1 - \frac{3\Gamma(\phi \to e^+e^-)\sqrt{s}}{\alpha D_\phi(s)}\right|^2 &(10)\\
&F(x,a,b) = \frac{2\alpha}{\pi(1-\xi)^{3/2}}\left\{\frac{3}{2}\left(a - \frac{a^3}{3}\right)F_1 + \frac{3}{4}a(1-a^2)F_2\right\}\\
&F_1 = \frac{1}{x}\left(x^2 - \frac{\xi(1-\xi)(1-x)}{(1-b^2)(1-x)+b^2\xi}\right)f(x) + (1-\xi)\left(1 - x - \frac{\xi}{2}\right)\frac{1}{x}\ln\frac{1+f(x)}{1-f(x)}\\
&F_2 = \frac{1}{x}\left(\frac{\xi^2(x-1)}{(1-b^2)(1-x)+b^2\xi} + 2x - 2 - x^2\right)f(x) + \xi\left(2 - x - \frac{\xi}{2}\right)\frac{1}{x}\ln\frac{1+f(x)}{1-f(x)}
\end{aligned}$$

where $f(x) = b\sqrt{1 - \frac{\xi}{1-x}}$. The nonradiative cross section $e^+e^- \to \pi^+\pi^-$ is:

$$\sigma_0(s) = \frac{\pi\alpha^2}{3s}(1-\xi)^{3/2}|F(s)|^2. \tag{11}$$

In the vector dominance model the form-factor is $|F(s)|^2 = (\frac{g_{\rho\pi\pi}}{f_\rho})^2\frac{m_\rho^4}{|D_\rho(s)|^2}$. We use for the form-factor in the ϕ meson region the expression:

$$|F(s)|^2 = 2,6\frac{|D_\rho(m_\phi)|^2}{|D_\rho(s)|^2}, \tag{12}$$

which describes the experimental data in the ϕ meson region $m_\rho^2 < s < 1,1\ GeV$ [19] reasonably good.

The interference between the amplitudes from Eqs. (2) and (8) is equal

$$\begin{aligned}
&\frac{d\sigma_{int}}{d\omega} = \frac{\alpha^3}{s\sqrt{s}}\left(\frac{g_{\rho\pi\pi}}{f_\rho}\right)\left(\frac{g_{f_0\pi\pi}}{f_\phi}\right)Re\left[\frac{m_\phi^2 m_\rho^2 g_R(t)}{\sqrt{4\pi\alpha}D_\phi D_\rho^* D_{f_0}}\left(1 - \frac{3\Gamma(\phi \to e^+e^-)\sqrt{s}}{\alpha D_\phi^*(s)}\right)\right] \times &(13)\\
&\times\left\{f(x) + \frac{\xi}{2}\ln\frac{1-f(x)}{1+f(x)}\right\}\left(a + \frac{a^3}{3}\right)
\end{aligned}$$

In the similar way let us give the expression for the differential cross section of the initial state radiation.

$$\frac{d\sigma_i}{d\omega} = 2\sigma_0(t)\frac{1}{\sqrt{s}}H(x,a,b)|1-\frac{3\Gamma(\phi\to e^+e^-)\sqrt{t}}{\alpha D_\phi(t)}|^2 \tag{14}$$
$$H(x,a,b) = \frac{\alpha}{\pi}\left[\left(\frac{2(1-x)+x^2}{x}\ln\frac{1+a}{1-a}-ax\right)(\frac{3b}{2}-\frac{b^3}{2})+\frac{3a(1-x)(b^3-b)}{x}\right]$$

Evaluating $H(x,a,b)$ we ignored the electron mass. At $b=1$ our result coincides with [17] (putting $\beta_e=1$) and differs by terms of order x with the result quoted by [15] [2].

Let us discuss the question about the radiative corrections to the studied processes. The corrections related to the final state are proportional to $L=\ln\frac{s}{m_\pi^2}\simeq 4$ and in the ϕ meson peak are small as compared with the initial state corrections which are proportional to $L=\ln\frac{s}{m_e^2}\simeq 16$. We take into account the corrections related with the initial state only. If to take into account that the initial state radiation is approximately twice the final state radiation at our angle cuts, see below, then we get that the radiative corrections to the final state radiation is about 10% of the ones to the initial state radiation. The general formulae are obtained in [20]. We consider approximate expressions only.

The total cross section of the one photon annihilation with the soft photon radiation and with the virtual corrections of order α is given by

$$\sigma(s) = \tilde{\sigma}(s)\{1+\frac{2\alpha}{\pi}[(L-1)\ln\frac{2\omega_{min}}{\sqrt{s}}+\frac{3}{4}L+\frac{\pi^2}{6}-1]\} \tag{15}$$
$$\tilde{\sigma}(s) = (\sigma_\phi(s)+\sigma_{int}(s)+\sigma_i+\sigma_f)\frac{1}{|1-\Pi(s)|^2}$$

where ω_{min} is the minimal photon energy registered, $L=\ln\frac{s}{m_e^2}$ is the "main" logarithm. The given expression is true under condition that ω_{min} is not larger than the typical resonant width Γ_{res}. In our case $\Gamma_{res}\gtrsim 25\ MeV$ and $\omega_{min}=20\ MeV$, so this condition holds. Much more exact expressions could be found in [20]. The electron vacuum polarization of order α is

---

[2] See the note in [17].

$$\Pi(s) = \frac{\alpha}{3\pi}(L - \frac{5}{3}) \tag{16}$$

where the contribution of muons and light hadrons is ignored. As one can see from (15) the radiation corrections lower the cross section by 20%.

II. PRODUCTION MODELS OF f_0 MESON.

We consider two models: i) the four-quark ($q^2\bar{q}^2$) model and ii) the model of the scalar $K\bar{K}$ molecule.

i) In the framework of the four-quark model the $f_0(980)$ meson is coupled strongly with the $K\bar{K}$ channel (OZI superallowed coupling constant). In the paper [9] the coupling constant of f_0 with K^+K^- was chosen:

$$\frac{g^2_{f_0K^+K^-}}{4\pi} = 2,3\ GeV^2, \tag{17}$$

but the other values $g^2_{f_0K^+K^-}/4\pi \simeq 1 - 4\ GeV^2$ are also acceptable. The relation $R = g^2_{f_0K^+K^-}/g^2_{f_0\pi^+\pi^-}$ is treated like a parameter of the model. The processes $\pi\pi \to \pi\pi$ and $\pi\pi \to K\bar{K}$ permit the wide enough range for R: $R = 4-10$. When $R = 8$, $g^2_{f_0K^+K^-}/4\pi = 2,3\ GeV^2$ we get $BR(\phi \to \gamma f_0 \to \gamma\pi\pi) = 2,3 \cdot 10^{-4}$ and effective (visible) width $\Gamma_{f_0} \simeq 25\ MeV$ [9].

In view of the strong coupling constant of the f_0 meson with the $K\bar{K}$ channel and the vicinity to the $K\bar{K}$ threshold it is necessary to take into account the finite width corrections in the propagator of the f_0 meson. Note, that the finite width corrections distort crucially the ordinary resonant Breit-Wigner formulae.

In the four-quark model we treat the propagator in following manner:

$$D_{f_0}(t) = m^2_{f_0} - t + Re\Pi_{f_0}(m^2_{f_0}) - \Pi_{f_0}(t), \tag{18}$$

where the term $Re\Pi_{f_0}(m^2_{f_0}) - \Pi_{f_0}(t)$ takes into account the finite width corrections [1,10]

$$\Pi_{f_0}(t) = \sum_{ab} \Pi^{ab}_{f_0}(t),$$

$$Im\Pi^{ab}_{f_0}(t) = \sqrt{t}\Gamma(f_0 \to ab, t) = \frac{g^2_{f_0ab}}{16\pi}\rho_{ab}(t),$$

$$\rho_{ab}(t) = \sqrt{\left(1 - \frac{m_+^2}{t}\right)\left(1 - \frac{m_-^2}{t}\right)}, \qquad m_\pm = m_a \pm m_b. \tag{19}$$

The final particle identity is taken into account in the definition of $g_{f_0 aa}$.

Let $m_a < m_b$, then for $t > m_+^2$

$$\Pi_{f_0}^{ab}(t) = \frac{g_{f_0 ab}^2}{16\pi}\left[L + \frac{1}{\pi}\rho_{ab}(t)\ln\frac{\sqrt{t - m_-^2} - \sqrt{t - m_+^2}}{\sqrt{t - m_-^2} + \sqrt{t - m_+^2}}\right] + i\sqrt{t}\Gamma(f_0 \to ab, t),$$
$$L = \frac{m_+ m_-}{\pi t}\ln(m_b/m_a). \tag{20}$$

For $m_-^2 < t < m_+^2$ [3]

$$\Pi_{f_0}^{ab}(t) = \frac{g_{f_0 ab}^2}{16\pi}\left[L - |\rho_{ab}(t)| + \frac{2}{\pi}|\rho_{ab}(t)|\arctan\frac{\sqrt{m_+^2 - t}}{\sqrt{t - m_-^2}}\right]. \tag{21}$$

For $t < m_-^2$

$$\Pi_{f_0}^{ab}(t) = \frac{g_{f_0 ab}^2}{16\pi}\left[L - \frac{1}{\pi}\rho(t)_{ab}\ln\frac{\sqrt{m_+^2 - t} - \sqrt{m_-^2 - t}}{\sqrt{m_+^2 - t} + \sqrt{m_-^2 - t}}\right]. \tag{22}$$

We consider the finite width corrections for the f_0 meson due to the $\pi\pi,\ K^+K^-, K^0\bar{K}^0,\ \eta\eta$ channels as in [9].

The calculation of the production amplitude $\phi \to \gamma f_0$ in the framework of the four-quark model gives the following expression for $g_R(t)$ [9]: when $t < 4m_{K^+}^2$

$$g_R(t) = \frac{e}{2(2\pi)^2} g_{f_0 K^+K^-} g_{\phi K^+K^-}\Bigg\{1 + \frac{1 - \rho^2(t)}{\rho(m_\phi^2)^2 - \rho(t)^2}\Bigg[2|\rho(t)|\arctan\frac{1}{|\rho(t)|} -$$
$$-\rho(m_\phi^2)\lambda(m_\phi^2) + i\pi\rho(m_\phi^2) - (1 - \rho^2(m_\phi^2))\left(\frac{1}{4}(\pi + i\lambda(m_\phi^2))^2 - \left(\arctan\frac{1}{|\rho(t)|}\right)^2\right)\Bigg]\Bigg\}, \tag{23}$$

where

$$\rho(t) = \sqrt{1 - \frac{4m_{K^+}^2}{t}} \qquad \lambda(t) = \ln\frac{1 + \rho(t)}{1 - \rho(t)}. \tag{24}$$

When $t > 4m_{K^+}^2$

---

[3] In paper [10] in (25) there is a misprint, the third term should have the positive sign, see (21).

$$g_R(t)=\frac{e}{2(2\pi)^2}g_{f_0K^+K^-}g_{\phi K^+K^-}\Bigg\{1+\frac{1-\rho^2(t)}{\rho(m_\phi^2)^2-\rho(t)^2}\Bigg[\rho(t)(\lambda(t)-i\pi)-$$

$$-\rho(m_\phi^2)(\lambda(m_\phi^2)-i\pi)-\frac{1}{4}(1-\rho^2(m_\phi^2))\Bigg((\pi+i\lambda(m_\phi^2))^2-(\pi+i\lambda(t))^2\Bigg)\Bigg]\Bigg\}. \qquad (25)$$

The coupling constant $g_{\phi K^+K^-}$ is related to the width:

$$\Gamma(\phi\to K^+K^-)=\frac{1}{3}\frac{g^2_{\phi K^+K^-}}{16\pi}m_\phi\rho(m_\phi)^3 \qquad (26)$$

ii) The coupling constant in the model of the scalar $K\bar{K}$ molecule [11]:

$$\frac{g^2_{f_0K^+K^-}}{4\pi}=0,6\ GeV^2. \qquad (27)$$

The coupling of the f_0 meson with the $K\bar{K}$ channel in the model of the $K\bar{K}$ molecule is considerably weaker than in the four-quark model.

In view of it, we use in the molecular model the propagator of the f_0 meson in the traditional Breit-Wigner form.

If $t>4m^2_{K^+}\ ,\ \ 4m^2_{K^0}\ ,$

$$\begin{aligned}D_{f_0}(t)&=M^2_{f_0}-t-i\sqrt{t}(\Gamma_0(t)+\Gamma_{K\bar{K}}(t))\\ \Gamma_{K\bar{K}}(t)&=\frac{g^2_{f_0K^+K^-}}{16\pi}(\sqrt{1-4m^2_{K^+}/t}+\sqrt{1-4m^2_{K^0}/t})\frac{1}{\sqrt{t}}\ .\end{aligned} \qquad (28)$$

If $4m^2_{K^+}<t<4m^2_{K^0}\ ,$

$$D_{f_0}(t)=M^2_{f_0}-t+\frac{g^2_{f_0K^+K^-}}{16\pi}\sqrt{4m^2_{K^0}/t-1}-i\frac{g^2_{f_0K^+K^-}}{16\pi}\sqrt{1-4m^2_{K^+}/t}-i\sqrt{t}\Gamma_0(t)\ . \qquad (29)$$

When $4m^2_{K^+}\ ,\ \ 4m^2_{K^0}>t\ ,$

$$D_{f_0}(t)=M^2_{f_0}-t+\frac{g^2_{f_0K^+K^-}}{16\pi}(\sqrt{4m^2_{K^+}/t-1}+\sqrt{4m^2_{K^0}/t-1})-i\sqrt{t}\Gamma_0(t), \qquad (30)$$

where the decay width of the scalar f_0 resonance into the $\pi\pi$ channel $\Gamma_0(t)$ is determined by Eq. (3).

As a parameter we use the decay width of resonance $\Gamma(f_0\to\pi\pi,m_{f_0})=\Gamma_0(m^2_{f_0})=\Gamma_0$. For $\Gamma_0=50\ MeV$ the effective (visible) width is $\simeq 25\ MeV$ and the branching ratio into the $K\bar{K}$ channel is $BR(f_0 \to K\bar{K}) \simeq 0,35$. For $\Gamma_0 = 100\ MeV$ the effective (visible) width is $\simeq 75\ MeV$ and the branching ratio into the $K\bar{K}$ channel is $BR(f_0 \to K\bar{K}) \simeq 0,3$.

Since the scalar resonance lies under the $K\bar{K}$ threshold, the peak in the cross section or in the mass spectrum does not coincide with M_{f_0}. It is easy to check using Eqs. (28)–(30). Because of this the mass in the Breit-Wigner formulas should be renormalized:

$$M_{f_0}^2 = m_{f_0}^2 - \frac{g_{f_0K^+K^-}^2}{16\pi}\left(\sqrt{4m_{K^+}^2/m_{f_0}^2 - 1} + \sqrt{4m_{K^0}^2/m_{f_0}^2 - 1}\right) , \tag{31}$$

where $m_{f_0}^2$ is the physical mass square and $M_{f_0}^2$ is the bare mass square. So, the physical mass is greater then the bare one. This fact is particularly important when the coupling of scalar meson with the $K\bar{K}$ channel is strong as it is in the four-quark and molecular models. But this circumstance was not taken into account neither in fitting data nor in theoretical papers with the exception of [1,9,10,12,18,21].

Let us note that Eqs. (28)–(30) are true in the resonance region only. They have wrong analytical properties at $t = 0$, for example. The expressions that are free of this trouble are given above, see Eqs. (18)–(22).

When the scalar resonance lies between the $K\bar{K}$ thresholds the renormalization of mass should be done in the following way:

$$M_{f_0}^2 = m_{f_0}^2 - \frac{g_{f_0K^+K^-}^2}{16\pi}\sqrt{4m_{K^0}^2/m_{f_0}^2 - 1} \ . \tag{32}$$

Note, that in the molecular model $m_{f_0} - M_{f_0} = 24(10)\ MeV$ for $m_{f_0} = 980(2m_{K^+})\ MeV$.

The calculation of the amplitude in the model of the scalar $K\bar{K}$ molecule was performed in [12]. As the analysis of model has shown the imaginary part of the production amplitude $\phi \to \gamma f_0$ gives about 90% of all intensity of the decay $\phi \to \gamma f_0 \to \gamma\pi\pi$. Therefore in the model of the scalar $K\bar{K}$ molecule we consider the imaginary part of $g_R(t)$ only.

When $t < 4m_{K^+}^2$

$$Img_R(t) = \pi e g_{f_0K^+K^-} g_{\phi K^+K^-} \frac{\mu^4}{(2\pi)^2}\frac{1}{(t-4a^2)^2}\left\{\frac{m_\phi^2}{\omega^3}\left(\ln\frac{(E_1-a)(E_2+a)}{(E_2-a)(E_1+a)} \times \right.\right.$$
$$\left. \times \frac{E_1E_2t(12a^2-t) - a^2m_\phi^2(t+4a^2)}{4a^3t}\right) + \frac{4m_{K^+}^2}{\sqrt{t}\omega}\ln\frac{E_1^2-a^2}{E_2^2-a^2} + \frac{8m_{K^+}^2}{\omega\sqrt{t}}\lambda(m_\phi^2) -$$

$$-\frac{m_\phi^2(t-4a^2)\rho(m_\phi^2)}{2a^2\omega^2}-\frac{32m_\phi^2\rho(m_\phi^2)^3(t-4a^2)^2}{3(m_\phi^2-4a^2)^3}\Bigg\} \tag{33}$$

where $a^2=m_{K^+}^2-\mu^2$, $p_0=(m_\phi^2+t)/2\sqrt{t}$, $\omega=(m_\phi^2-t)/2\sqrt{t}$, $E_1=\frac{1}{2}(p_0-\omega\rho(m_\phi^2))$, and $E_2=\frac{1}{2}(p_0+\omega\rho(m_\phi^2))$.

When $t>4m_{K^+}^2$

$$\begin{aligned} Img_R(t)=\pi e g_{f_0K^+K^-}g_{\phi K^+K^-}\frac{\mu^4}{(2\pi)^2}\frac{1}{(t-4a^2)^2}\Bigg\{\frac{m_\phi^2}{\omega^3}\Bigg(\ln\frac{(E_1-a)(E_2+a)}{(E_2-a)(E_1+a)}\times \\ \times\frac{E_1E_2t(12a^2-t)-a^2m_\phi^2(t+4a^2)}{4a^3t}\Bigg)+\frac{4m_{K^+}^2}{\omega\sqrt{t}}\ln\frac{E_1^2-a^2}{E_2^2-a^2}+\frac{8m_{K^+}^2}{\omega\sqrt{t}}\lambda(m_\phi^2)- \\ -\frac{m_\phi^2(t-4a^2)\rho(m_\phi^2)}{2a^2\omega^2}-\frac{32m_\phi^2\rho(m_\phi^2)^3(t-4a^2)^2}{3(m_\phi^2-4a^2)^3}+\frac{4m_\phi^2\rho(t)}{\omega\sqrt{t}}-\frac{8m_{K^+}^2}{\omega\sqrt{t}}\lambda(t)\Bigg\} \end{aligned} \tag{34}$$

where $\mu=140\ MeV$ [11].

For the propagator of the ϕ meson we use the expression:

$$D_\phi(s)=m_\phi^2-s-is\frac{g_{\phi K^+K^-}^2}{48\pi}\left[(1-\frac{4m_{K^+}^2}{s})^{3/2}+c_1(1-\frac{4m_{K^0}^2}{s})^{3/2}\right]-ic_2p_{\pi\rho}^3(s) \tag{35}$$

where $p_{\pi\rho}^2(s)=\sqrt{s}\rho_{\pi\rho}(s)/2$. Taking into account the branching ratios of the ϕ meson decays and the total normalization we get $c_1=1,09$ and $c_2=0,1$.

The propagator of the ρ meson is:

$$D_\rho(s)=m_\rho^2-s-is\frac{g_{\rho\pi\pi}^2}{48\pi}(1-\frac{4m_\pi^2}{s})^{3/2} \tag{36}$$

III. THE INTERFERENCE PATTERNS.

We consider the following parameters in the four-quark model: $m_{f_0}=980\ MeV$, $R=8$, $g_{f_0K^+K^-}^2/4\pi=2,3\ GeV^2$, so that $BR(\phi\to\gamma f_0\to\gamma\pi\pi)=2,3\cdot10^{-4}$ and the visible width $\Gamma_{f_0}\simeq25\ MeV$ [9]. The interference pattern by the total energy of the beams in the full cross section of the reaction $e^+e^-\to\gamma\pi^+\pi^-$, $\sigma=\sigma_\phi\pm\sigma_{int}+\sigma_f+\sigma_i$, at the ϕ peak is shown in Fig.2. Guided by [13], we choose the angle cuts $a=0,66$ and $b=0.955$, which decrease the initial state radiation by a factor of nine. But, in despite of the strong suppression, the initial state radiation stays dominant and is equal about $\frac{2}{3}$ of total background. The energy of the photon lies in the interval $20 < \omega < 100\ MeV$.

The dotted line and the line 1 apply to the pure background and to the background with the $\phi - \rho$ transition respectively. The lines 2 and 3 show constructive and destructive interference correspondingly.

As one can see from Eq. (9) the contribution of the $\phi - \rho$ transition to the amplitude is about 15% at $\sqrt{s} = m_\phi \pm \Gamma_\phi/2$. But, since the initial state radiation, in which the $\phi - \rho$ transition is negligible for the $\sqrt{t} < m_\phi - 20\ MeV$, forms the major part of background the relative contribution of $\phi - \rho$ transition is smaller in the total pattern than in the $e^+e^- \to \pi^+\pi^-$ one and is equal about 4% at $\sqrt{s} = m_\phi \pm \Gamma_\phi/2$, as it is seen from Fig.2.

The interference pattern in the photon spectrum $d\sigma_\phi/d\omega \pm d\sigma_{int}/d\omega$ at the ϕ meson point is shown in Fig.3.

In the model of the scalar $K\bar{K}$ molecule we use the parameter: $\Gamma(f_0 \to \pi\pi, m_{f_0} = 980\ MeV) = \Gamma_0 = 50\ MeV$. For $m_{f_0} = 980\ MeV$, $g^2_{f_0K^+K^-}/4\pi = 0,6\ GeV^2$ we have $BR(\phi \to \gamma f_0 \to \gamma\pi\pi) = 1,7 \cdot 10^{-5}$ [12]. The visible width is $\simeq 25\ MeV$ and the branching ratio into the $K\bar{K}$ channel is $BR(f_0 \to K\bar{K}) \simeq 0,35$. The angle cuts are the same. The interference patterns are shown in Fig.4 and Fig.5.

IV. CONCLUSION.

The analysis of the graphs presented shows that the observation of the interference patterns in the reaction $e^+e^- \to \gamma\pi^+\pi^-$ is quite possible at the building ϕ-factories in Novosibirsk and Frascati. In the case of $q^2\bar{q}^2$ model the observation is possible at the detectors CMD-2 and SND at the VEPP-2M collider. Furthermore, the planed experimental statistics at the ϕ-factories will let analyzing interference patterns to decide between two models of the f_0 meson makeup: $q^2\bar{q}^2$ model and the model of the $K\bar{K}$ molecule.

Really, as one can see in Fig.2, in the case of $q^2\bar{q}^2$ model the difference between the constructive interference and the background at the ϕ meson point is $\simeq 0,34\ nb$, and for the destructive interference this difference is $\simeq 0,14$ *nb*, at the total cross section $e^+e^- \to \gamma\pi^+\pi^-$ is $1,6$ *nb*.

As it is seen from Fig.4, for the model of the $K\bar{K}$ molecule the difference between the destructive interference and the background equals approximately to the difference between the background and the constructive one and is $\simeq 0,07$ *nb* at the ϕ meson point.

Besides that, the comparison of two graphs shows that the behavior of the constructive interference in the $q^2\bar{q}^2$ case and in the case of the $K\bar{K}$ molecule differs fundamentally. In the $q^2\bar{q}^2$ case the constructive interference has a prominent peak while in the case of the $K\bar{K}$ molecule such a peak is absent. This behavior is easy to be distinguished experimentally since the difference of the cross sections is $0,27$ *nb*.

For the destructive interference the difference between two models is not so strong. In despite of the fact that the signal in the model of the scalar $K\bar{K}$ molecule is much weaker then in the $q^2\bar{q}^2$ model ($BR(\phi \to \gamma f_0(molecule) \to \gamma\pi\pi) \simeq \frac{1}{10}BR(\phi \to \gamma f_0(q^2\bar{q}^2) \to \gamma\pi\pi)$, see also [9,12], the cross section difference decreases not so much. The reason is that in the case of the destructive interference the interference term in the $q^2\bar{q}^2$ model is compensated by the modulus square of f_0 meson production amplitude meanwhile in the model of the $K\bar{K}$ molecule the interference term is dominant.

The difference between the cross sections of the destructive interference case in the four-quark model and in the model of the $K\bar{K}$ molecule is about 0.1 *nb* at the ϕ meson peak.

On the other hand, we have to note a quite week dependence of the interference pattern in the total cross section on the parameters of the models. To illustrate it we show the lines of the destructive interference for the different parameters of the models in Fig.6.

In the four-quark model for $m_{f_0} = 980\ MeV$, $R = 8$, $g^2_{f_0 K^+K^-}/4\pi = 2,3\ GeV^2$, so that $BR(\phi \to \gamma f_0 \to \gamma\pi\pi) = 2.3 \cdot 10^{-4}$, $BR(\phi \to \gamma f_0 \to \gamma\pi\pi, 20 < \omega < 100\ MeV) = 1.13 \cdot 10^{-4}$, the visible width $\Gamma_{f_0} \simeq 25\ MeV$ the curve is shown as a solid line.

The dotted line is for $m_{f_0} = 980\ MeV$, $R = 4$, $g^2_{f_0 K^+K^-}/4\pi = 4\ GeV^2$, so that $BR(\phi \to \gamma f_0 \to \gamma\pi\pi) = 5 \cdot 10^{-4}$, $BR(\phi \to \gamma f_0 \to \gamma\pi\pi, 20 < \omega < 100\ MeV) = 1.14 \cdot 10^{-4}$ and the visible width $\Gamma_{f_0} \simeq 50\ MeV$ in the four-quark model.

The dashed line for $m_{f_0} = 980\ MeV$, $R = 1$, $g^2_{f_0 K^+K^-}/4\pi = 0,19\ GeV^2$ that correspond the $s\bar{s}$ structure of the f_0 meson [9,10]. At such parameters $BR(\phi \to \gamma f_0 \to \gamma\pi\pi) = 5\cdot 10^{-5}$, $BR(\phi \to \gamma f_0 \to \gamma\pi\pi, 20 < \omega < 100\ MeV) = 2.4\cdot 10^{-5}$ and the visible width $\Gamma_{f_0} \simeq 50\ MeV$.

And also the curve without f_0 resonance (the line 2), we have for that $BR(\phi \to \gamma \to \rho \to \gamma\pi\pi, 20 < \omega < 100\ MeV) = 3,5\cdot 10^{-6}$, see appendix.

In despite of the fact that the values of the partial widths vary by two orders the total interference pattern changes not so dramatically.

In parallel with the interference pattern in the total cross section one should consider the interference pattern in the photon spectrum which for the visible width $\Gamma_{f_0} \simeq 25\ MeV$ has a good sensitivity since it is a differential characteristic, see Fig.3 and Fig.5. The concurrent observation of two interference patterns, by the energy of beam and by the energy of the photon, extends the possibility for analysis and allows to have more strong limits. Along with it, for the broad f_0 meson (the visible width $\Gamma_{f_0} \simeq 50\ MeV$) the interference pattern in the photon spectrum is less informative.

V. APPENDIX.

In the case of an experimental difficulties to distinguish the charged pions from muons the detected events $e^+e^- \to \gamma\pi^+\pi^-$ contain the part of the events from the reaction $e^+e^- \to \gamma\mu^+\mu^-$, [13]. In this situation it is important to know the cross section $\sigma(e^+e^- \to \gamma\mu^+\mu^-)$ and the branching ratio of the ϕ meson decay into the $\gamma\mu^+\mu^-$. In this appendix we give the necessary expressions and the values for $BR(\phi \to \gamma^* \to \gamma\mu^+\mu^-)$ and $BR(\phi \to \gamma^* \to \rho \to \gamma\pi^+\pi^-)$.

The cross section of the $e^+e^- \to \gamma\mu^+\mu^-$ process consists of the initial electron radiation, see Eq. (14):

$$\frac{d\sigma_i(e^+e^- \to \gamma\mu^+\mu^-)}{d\omega} = 2\sigma_0(t)\frac{1}{\sqrt{s}}H(x,a,b)|1 - \frac{3\Gamma(\phi \to e^+e^-)\sqrt{t}}{\alpha D_\phi(t)}|^2 \tag{37}$$

where the cross section of the $e^+e^- \to \mu^+\mu^-$ reaction

$$\sigma_0(s) = \frac{4\pi\alpha}{3s}\sqrt{1-\xi_\mu}(1+\frac{\xi_\mu}{2}), \tag{38}$$

we use the definitions: $\xi_\mu = 4\mu^2/s$, and the final muon radiation [22]:

$$\frac{d\sigma_f(e^+e^- \to \gamma\mu^+\mu^-)}{d\omega} = 2\sigma_0(s)\frac{1}{\sqrt{s}}F_\mu(x,a)|1 - \frac{3\Gamma(\phi \to e^+e^-)\sqrt{s}}{\alpha D_\phi(s)}|^2, \tag{39}$$

where

$$F_\mu(x,a) = \frac{3\alpha}{4\pi\sqrt{1-\xi_\mu}(1+\frac{\xi_\mu}{2})}\Big[-a(x+\frac{1-x}{x}\xi_\mu)f_\mu - \frac{a^3}{3}(x+\frac{1-x}{x}(8+\xi_\mu))f_\mu + \tag{40}$$
$$+a(x+\frac{1-x}{x}(2+\xi_\mu) - \frac{\xi_\mu}{x}(1+\frac{\xi_\mu}{2}))\ln\frac{1+f_\mu}{1-f_\mu} + \frac{a^3}{3}(x+\frac{1-x}{x}(2+\xi_\mu) +$$
$$+\frac{\xi_\mu}{x}(1-\frac{\xi_\mu}{2}))\ln\frac{1+f_\mu}{1-f_\mu}\Big].$$

and $f_\mu = \sqrt{1-\xi_\mu/(1-x)}$, see Fig.1g.

The sum of the initial electron radiation and the final muon radiation at $a = 0.66$ and $20 < \omega < 100\ MeV$ is shown in Fig.7. The initial radiation is about a half of the total background, in view of this the $\phi - \gamma$ contribution is suppressed relatively less than in the $e^+e^- \to \gamma\pi^+\pi^-$ process and is equal about 7% at $\sqrt{s} = m_\phi \pm \Gamma_\phi/2$.

The decay width $\phi \to \gamma^* \to \gamma\mu^+\mu^-$ is given in the following way:

$$\frac{d}{d\omega}\Gamma(\phi \to \gamma\mu^+\mu^-) = \frac{2}{m_\phi}\Gamma(\phi \to \mu^+\mu^-)F_\mu(x) \tag{41}$$

where

$$\Gamma(\phi \to \mu^+\mu^-) = \Gamma(\phi \to e^+e^-)(1+\frac{2\mu^2}{m_\phi^2})\sqrt{1-\frac{4mu^2}{m_\phi^2}} \tag{42}$$

and $F_\mu(x) = F_\mu(x, a=1)$.

After integrating over photon energy in the range $20 < \omega < 100$ ($\omega_{max} \simeq 470\ MeV$) we get:

$$BR(\phi \to \gamma\mu^+\mu^-) = 7,3 \cdot 10^{-6}(1,15 \cdot 10^{-5}). \tag{43}$$

Analogously the decay width $\phi \to \gamma^* \to \rho \to \gamma\pi^+\pi^-$ is given in the form:

$$\frac{d}{d\omega}\Gamma(\phi \to \gamma\pi^+\pi^-) = \frac{2}{m_\phi}\Gamma(\phi \to \pi^+\pi^-)F(x) \tag{44}$$

where $F(x) = F(x, a = 1, b = 1)$, see Eq. (10), and

$$\Gamma(\phi \to \pi^+\pi^-) = \frac{1}{4}\Gamma(\phi \to e^+e^-)(1 - \frac{4m_\pi^2}{m_\phi^2})^{3/2}|F(m_\phi^2)|^2. \tag{45}$$

The form-factor $|F(m_\phi^2)|^2 = 2,6$, see Eq. (12). After integrating in the range $20 < \omega < 100$ ($\omega_{max} \simeq 470\ MeV$) we get:

$$BR(\phi \to \gamma\pi^+\pi^-) = 3,5 \cdot 10^{-6}(4,7 \cdot 10^{-6}). \tag{46}$$

REFERENCES

[1] N.N. Achasov, S.A. Devyanin and G.N. Shestakov, Usp. Fiz. Nauk. **142**, 361 (1984).

[2] N.N. Achasov, Nucl. Phys. B (Proc. Suppl.) **21**, 189 (1991).

[3] N.N. Achasov and G.N. Shestakov, Usp. Fiz. Nauk **161**, 53 (1991).

[4] R.L. Jaffe, Phys. Rev. **D15**, 267, 281 (1977).

[5] J. Weinstein and N. Isgur, Phys. Rev. **D41**, 2236 (1990).

[6] N.A. Tӧrnqvist Phys. Rev. Lett., **49**, 624 (1982).

[7] N. Brown and F.E. Close, *THE DAΦNE PHYSICS HANDBOOK*, Vol. II, edited by L. Maiani, G. Pancheri, N. Paver, dei Laboratory Nazionali di Frascati, Frascati, Italy (December 1992), p. 447.

[8] F.E. Close, Yu.L. Dokshitzer, V.N. Gribov, V.A. Khoze and M.G. Ryskin, Phys. Lett. **B319**, 291 (1993).

[9] N.N. Achasov and V.N.Ivanchenko, Nucl. Phys. **B315**,465 (1989), Preprint INP 87-129 (1987), Novosibirsk.

[10] N.N. Achasov, *THE SECOND DAΦNE PHYSICS HANDBOOK*, Vol. II, edited by L. Maiani, G. Pancheri, N. Paver, dei Laboratory Nazionali di Frascati, Frascati, Italy (May 1995), p. 671.

[11] F.E. Close, N. Isgur and S. Kumano, Nucl. Phys. **B389**, 513 (1993).

[12] N.N. Achasov, V.V. Gubin and V.I. Shevchenko, hep-ph/9605245, to be published in Yad. Fiz.

[13] R.R. Akhmetshin et al., preprint Budker INP 95-62, 1995.

[14] M.N. Achasov et al., preprint Budker INP 96-47, 1996.

[15] A.Bramon, G.Colangelo and M.Greco, Phys.Lett. **287**, 263 (1992).

A.Bramon et al., *The DAΦNE Physics Handbook*, eds. L.Maiani, G.Pancheri and N.Paver, Vol. II, p. 487.

A.Bramon, M.Greco, *The second DAΦNE Physics Handbook*, eds. L.Maiani, G.Pancheri and N.Paver, Vol. II, p. 663.

[16] J. Lee-Franzini, W.Kim, P.J.Franzini,*The DAΦNE Physics Handbook*, eds. L.Maiani, G.Pancheri and N.Paver, Vol. II, p. 513.

J. Lee-Franzini, W.Kim, P.J.Franzini, preprint LNF-92/026 (R), 9 Aprile 1992.

G.Colangelo, P.J.Franzini, preprint LNF-92/058 (P), 22 Giugno 1992.

[17] J.L.Lucio M., M. Napsuciale, Phys.Lett. **B331**, 418 (1994).

[18] N.N. Achasov and V.V. Gubin, Phys. Lett. **B 363**, 106 (1995).

[19] A.D. Bukin et al., Yad. Fiz. **27**, 985 (1978).

[20] E.Kuraev and V.S.Fadin, Yad. Fiz. **41**, 733 (1985).

[21] N.N. Achasov and G.N. Shestakov, Z. Phys. **C41**, 309 (1988).

[22] V.N. Baier and V.A. Khose, Zh. Eksp. Teor. Fiz. **48**, 946, 1708 (1965).

FIGURES

FIG. 1. Model diagrams.

FIG. 2. The interference pattern in the total cross section: $\sigma = \sigma_\phi \pm \sigma_{int} + \sigma_f + \sigma_i$ for the $q^2\bar{q}^2$ model. $R = 8$, $g^2_{f_0 K^+K^-}/4\pi = 2{,}3\ GeV^2$, $BR(\phi \to \gamma f_0 \to \gamma\pi\pi) = 2{,}3 \cdot 10^{-4}$, $BR(\phi \to \gamma f_0 \to \gamma\pi\pi, 20 < \omega < 100\ MeV) = 1{,}3 \cdot 10^{-4}$, the visible width is 25 MeV. Dotted line is the pure background, the line 1 is the background with the $\phi - \rho$ transition, the line 2 is the constructive interference, the line 3 is the destructive one.

FIG. 3. The interference pattern in the photon spectrum: $d\sigma_\phi/d\omega \pm d\sigma_{int}/d\omega$ for the $q^2\bar{q}^2$ model. $R = 8$, $g^2_{f_0 K^+K^-}/4\pi = 2{,}3\ GeV^2$, $BR(\phi \to \gamma f_0 \to \gamma\pi\pi) = 2{,}3 \cdot 10^{-4}$. $BR(\phi \to \gamma f_0 \to \gamma\pi\pi, 20 < \omega < 100\ MeV) = 1{,}3 \cdot 10^{-4}$, the visible width is 25 MeV. The line 1 is the destructive interference, the line 2 is the constructive one.

FIG. 4. The interference pattern in the total cross section for the model of the $K\bar{K}$ molecule. $\Gamma(f_0 \to \pi\pi, m_{f_0} = 980\ MeV) = \Gamma_0 = 50\ MeV$, the visible width is 25 MeV. $BR(\phi \to \gamma f_0 \to \gamma\pi\pi) = 1{,}7 \cdot 10^{-5}$, $BR(\phi \to \gamma f_0 \to \gamma\pi\pi, 20 < \omega < 100\ MeV) = 1{,}4 \cdot 10^{-5}$. The dotted line is the pure background, the dashed line is the background with the $\phi - \rho$ transition, the line 1 is the constructive interference, the line 2 is the destructive one.

FIG. 5. The interference pattern in the photon spectrum for the model of the $K\bar{K}$ molecule. $\Gamma(f_0 \to \pi\pi, m_{f_0} = 980\ MeV) = \Gamma_0 = 50\ MeV$, the visible width is o25 MeV. $BR(\phi \to \gamma f_0 \to \gamma\pi\pi) = 1{,}7 \cdot 10^{-5}$, $BR(\phi \to \gamma f_0 \to \gamma\pi\pi, 20 < \omega < 100\ MeV) = 1{,}4 \cdot 10^{-5}$. The line 1 is the destructive interference, the line 2 is the constructive one.

FIG. 6. The interference pattern in the total cross section at the different parameters. The line 1 is the pure background. The line 2 is the background with the $\phi - \rho$ transition, $BR(\phi \to \gamma\pi^+\pi^-, 20 < \omega < 100) = 3,5 \cdot 10^{-6}$. The dotted line is the destructive interference for $R = 4$, $g^2_{f_0 K^+K^-}/4\pi = 4\ GeV^2$, $BR(\phi \to \gamma f_0 \to \gamma\pi\pi) = 5 \cdot 10^{-4}$, $BR(\phi \to \gamma f_0 \to \gamma\pi\pi, 20 < \omega < 100\ MeV) = 1,14 \cdot 10^{-4}$, the visible width $\Gamma_{f_0} = 50\ MeV$. The solid line is the destructive interference for $BR(\phi \to \gamma f_0 \to \gamma\pi\pi) = 2,3 \cdot 10^{-4}$, $BR(\phi \to \gamma f_0 \to \gamma\pi\pi, 20 < \omega < 100\ MeV) = 1,13 \cdot 10^{-4}$, the visible width $\Gamma_{f_0} = 25\ MeV$, see Fig.2. The dashed line is the destructive interference for $R = 1$, $g^2_{f_0 K^+K^-}/4\pi = 0,19\ GeV^2$, $BR(\phi \to \gamma f_0 \to \gamma\pi\pi) = 5 \cdot 10^{-5}$, $BR(\phi \to \gamma f_0 \to \gamma\pi\pi, 20 < \omega < 100\ MeV) = 2,4 \cdot 10^{-5}$, the visible width $\Gamma_{f_0} = 50\ MeV$.

FIG. 7. The $e^+e^- \to \gamma\mu^+\mu^-$ background. The sum of the initial electron radiation and the final muon one.

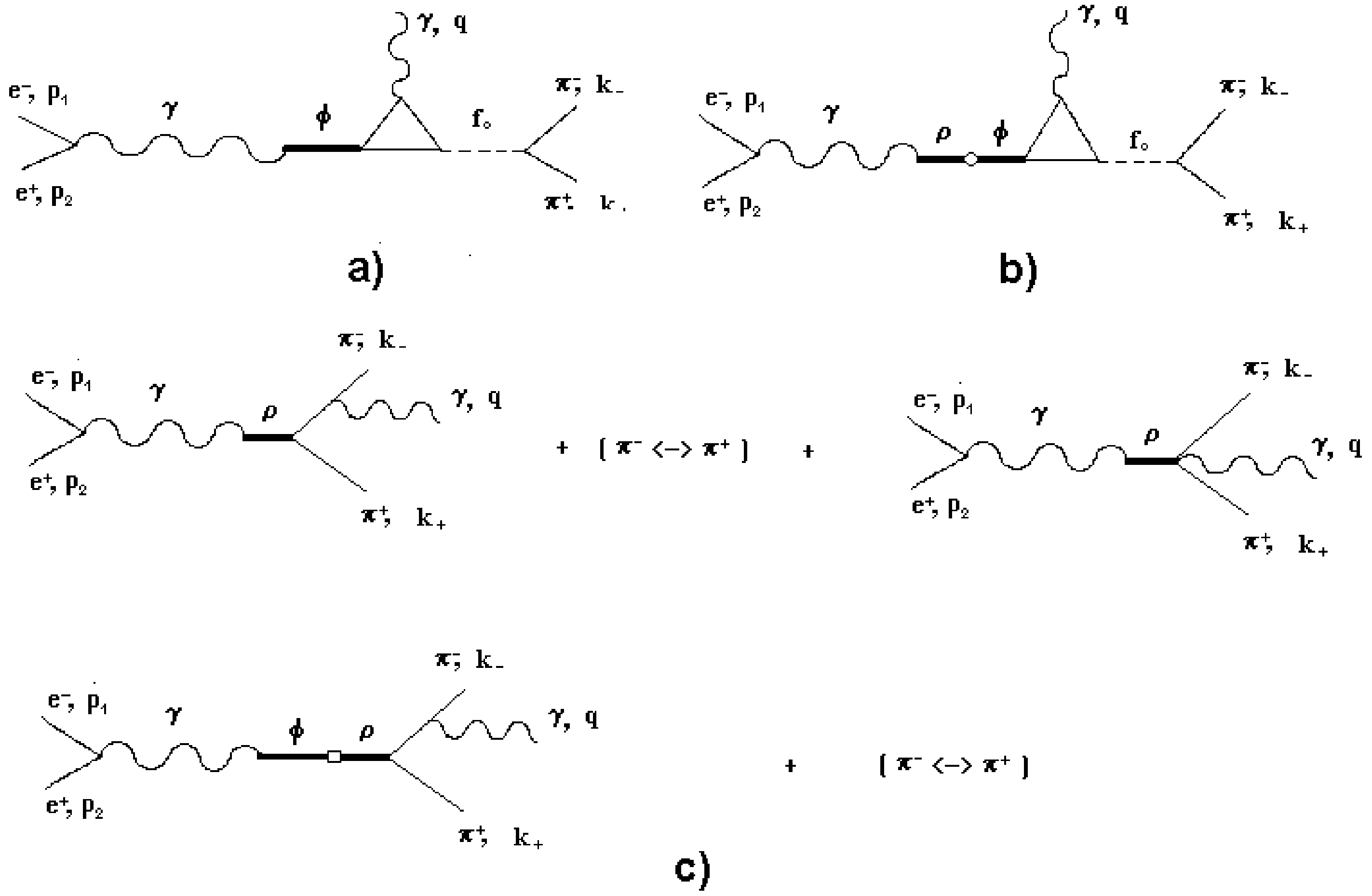
a)
e⁻, p₁
e⁺, p₂
γ
ϕ
γ, q
f₀
π⁻, k₋
π⁺, k₊
b)
e⁻, p₁
e⁺, p₂
γ
ρ
ϕ
γ, q
f₀
π⁻, k₋
π⁺, k₊
c)
e⁻, p₁
e⁺, p₂
γ
ρ
π⁻, k₋
γ, q
π⁺, k₊
+ (π⁻ <-> π⁺) +
e⁻, p₁
e⁺, p₂
γ
ρ
π⁻, k₋
γ, q
π⁺, k₊
e⁻, p₁
e⁺, p₂
γ
ϕ
ρ
π⁻, k₋
γ, q
π⁺, k₊
+ (π⁻ <-> π⁺)

Fig. 1

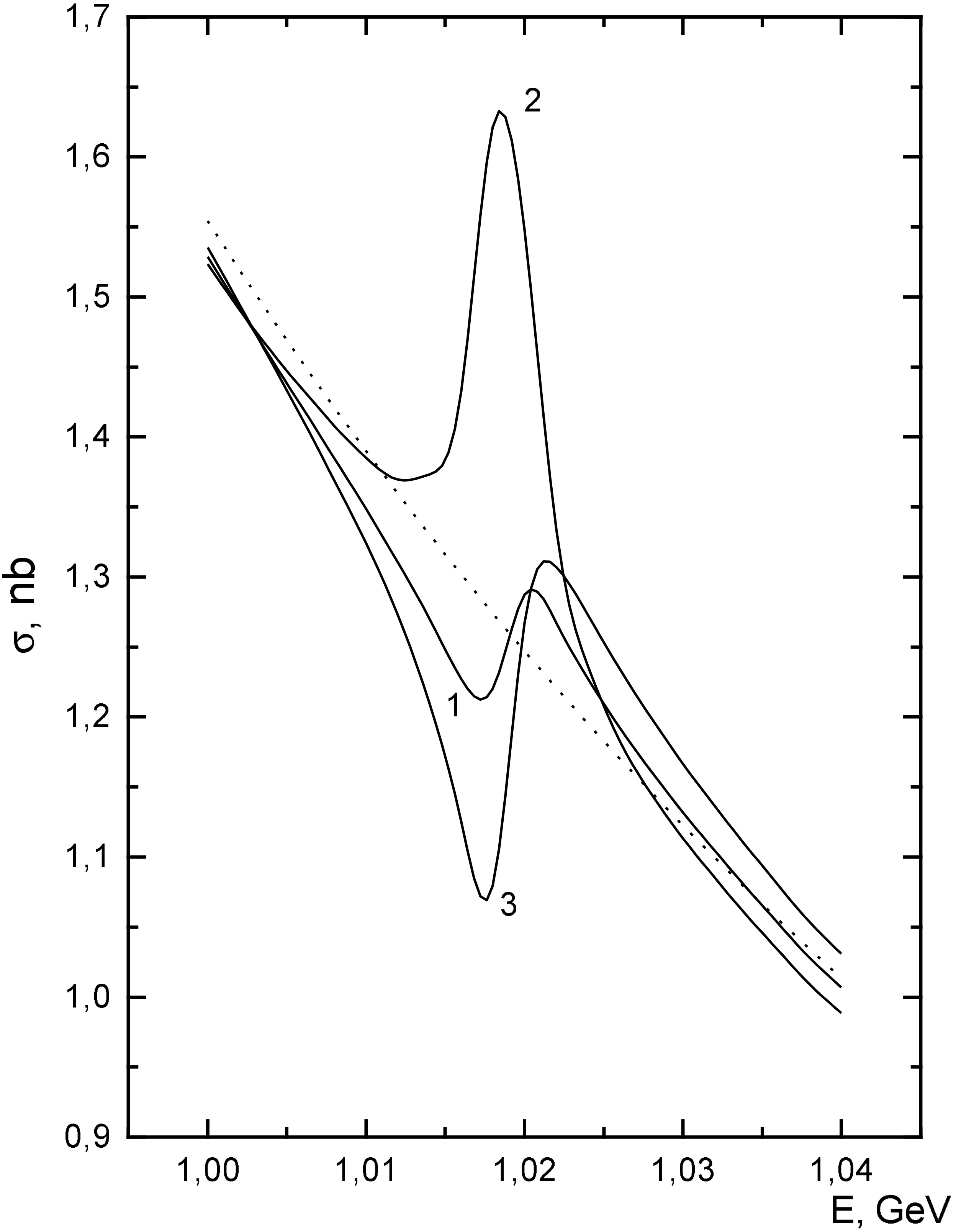

Fig. 2

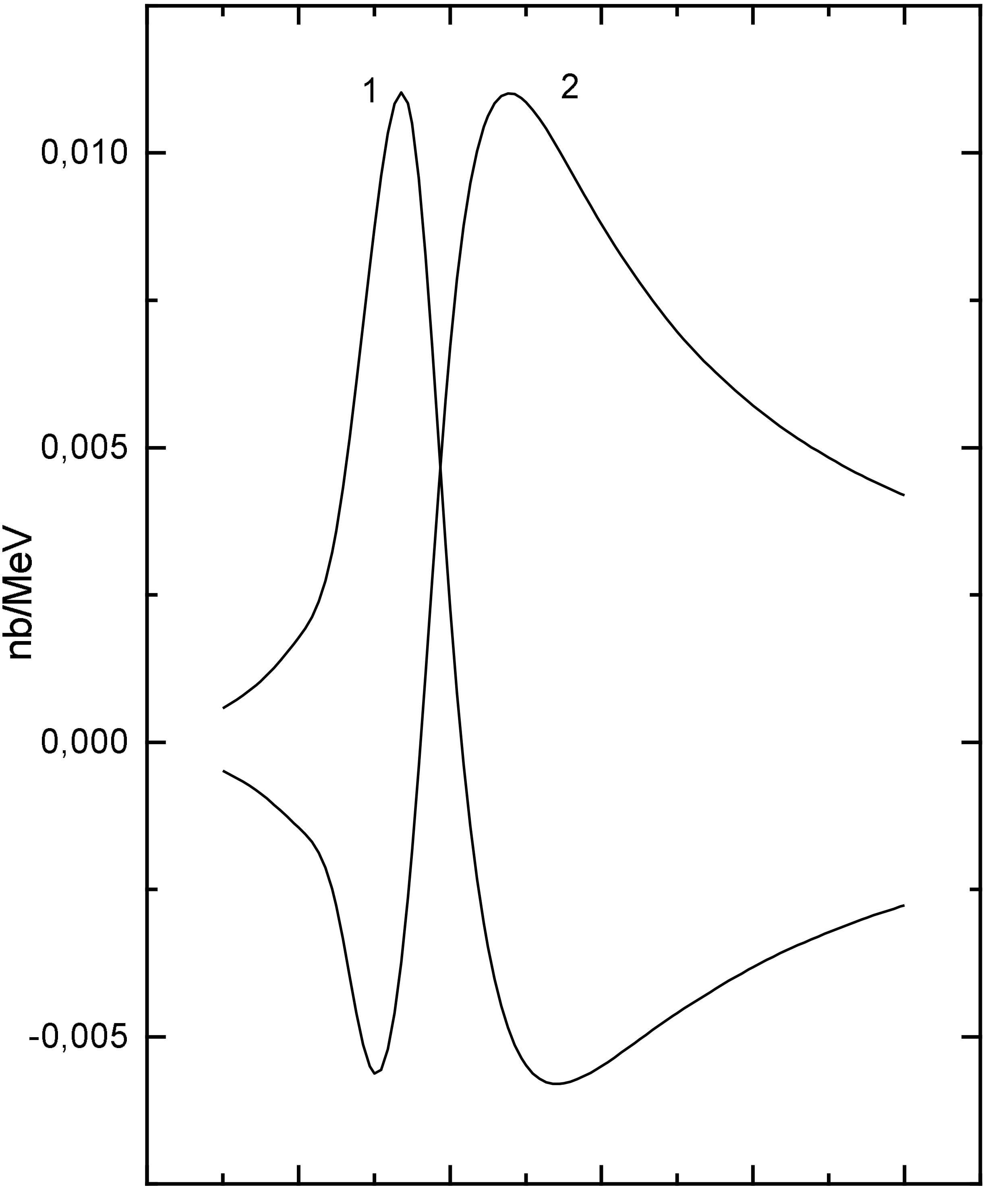

Fig. 3

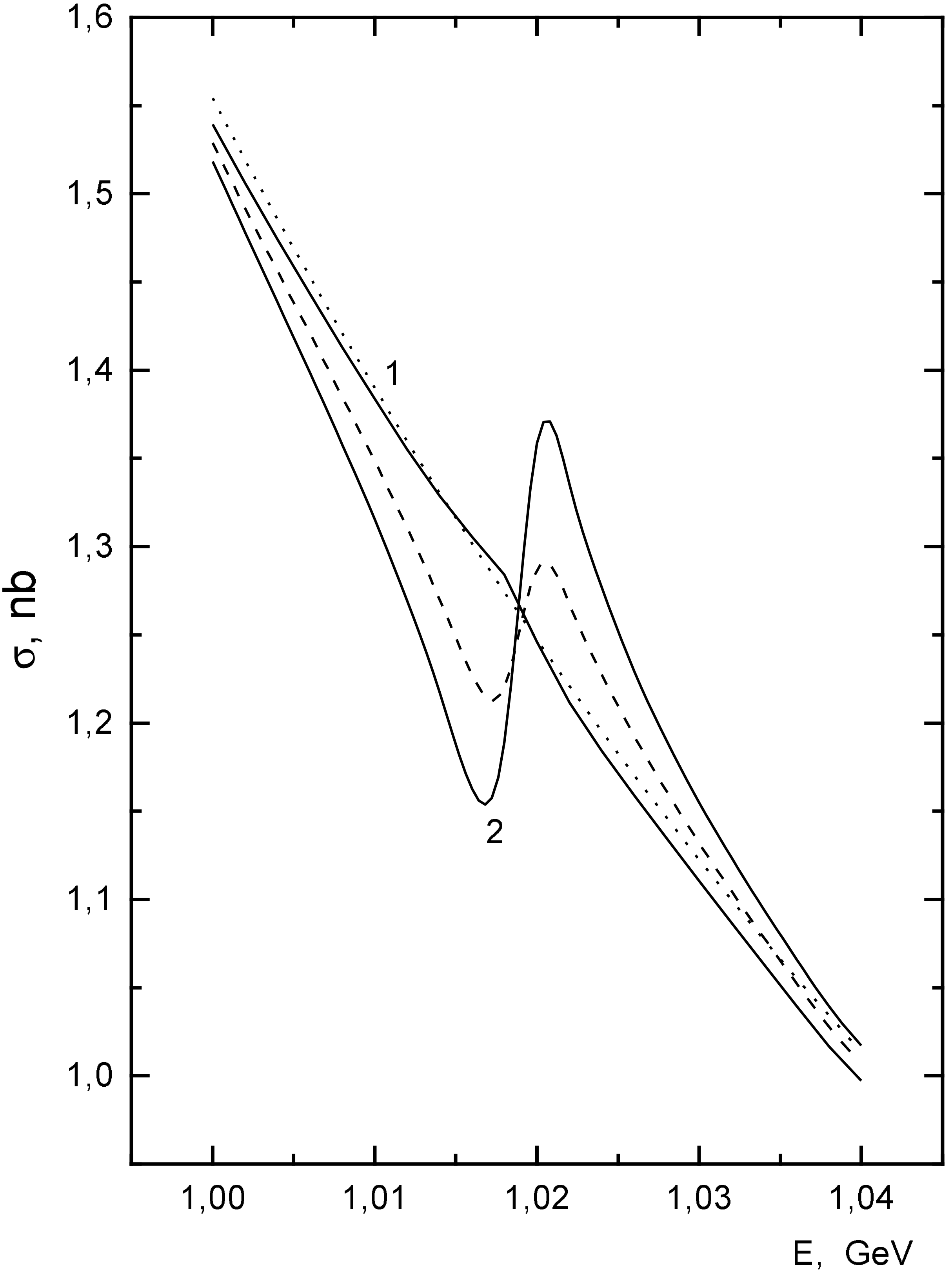

Fig. 4

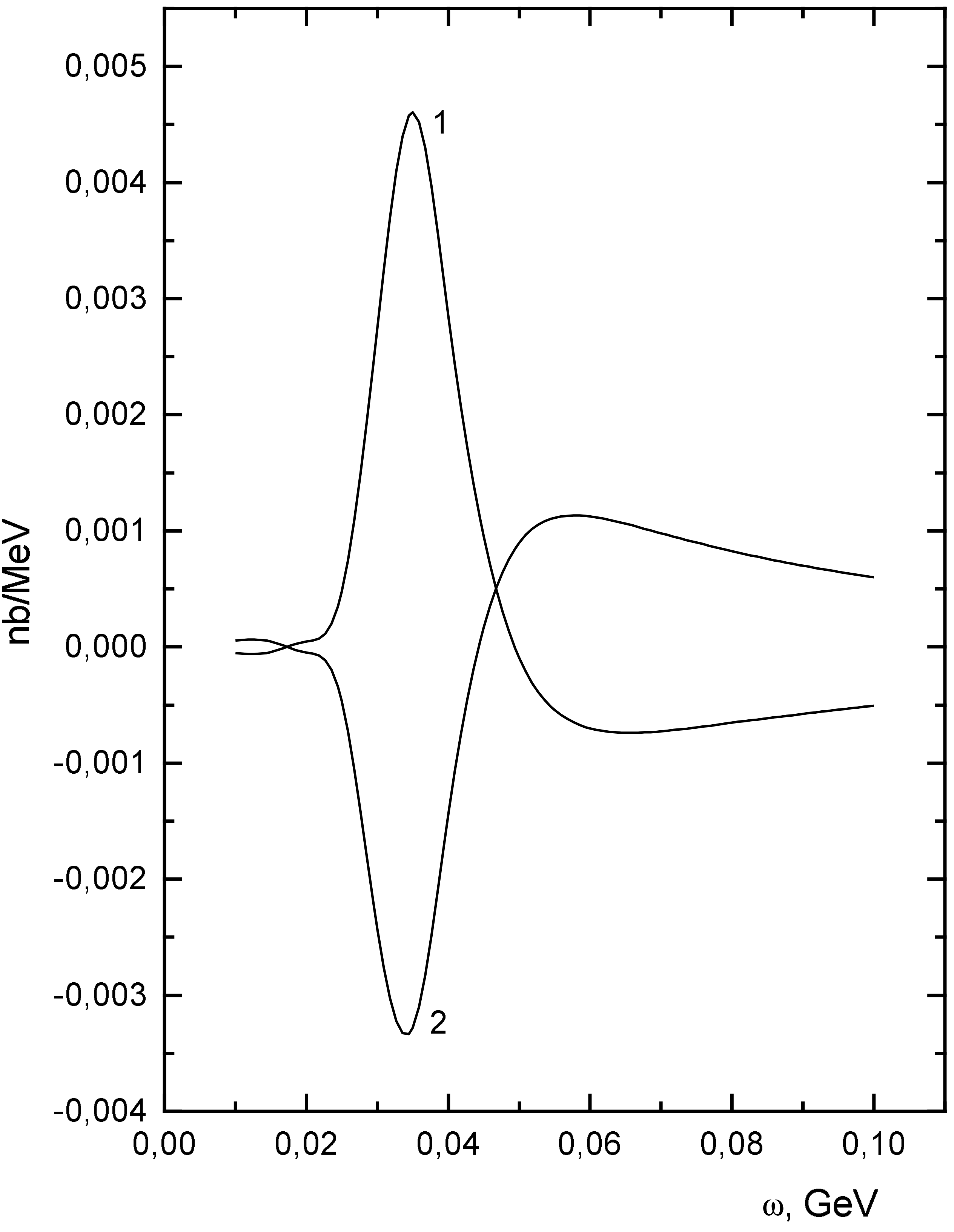
nb/MeV
0,005
0,004
0,003
0,002
0,001
0,000
-0,001
-0,002
-0,003
-0,004
0,00
0,02
0,04
0,06
0,08
0,10
ω, GeV
1
2

Fig. 5

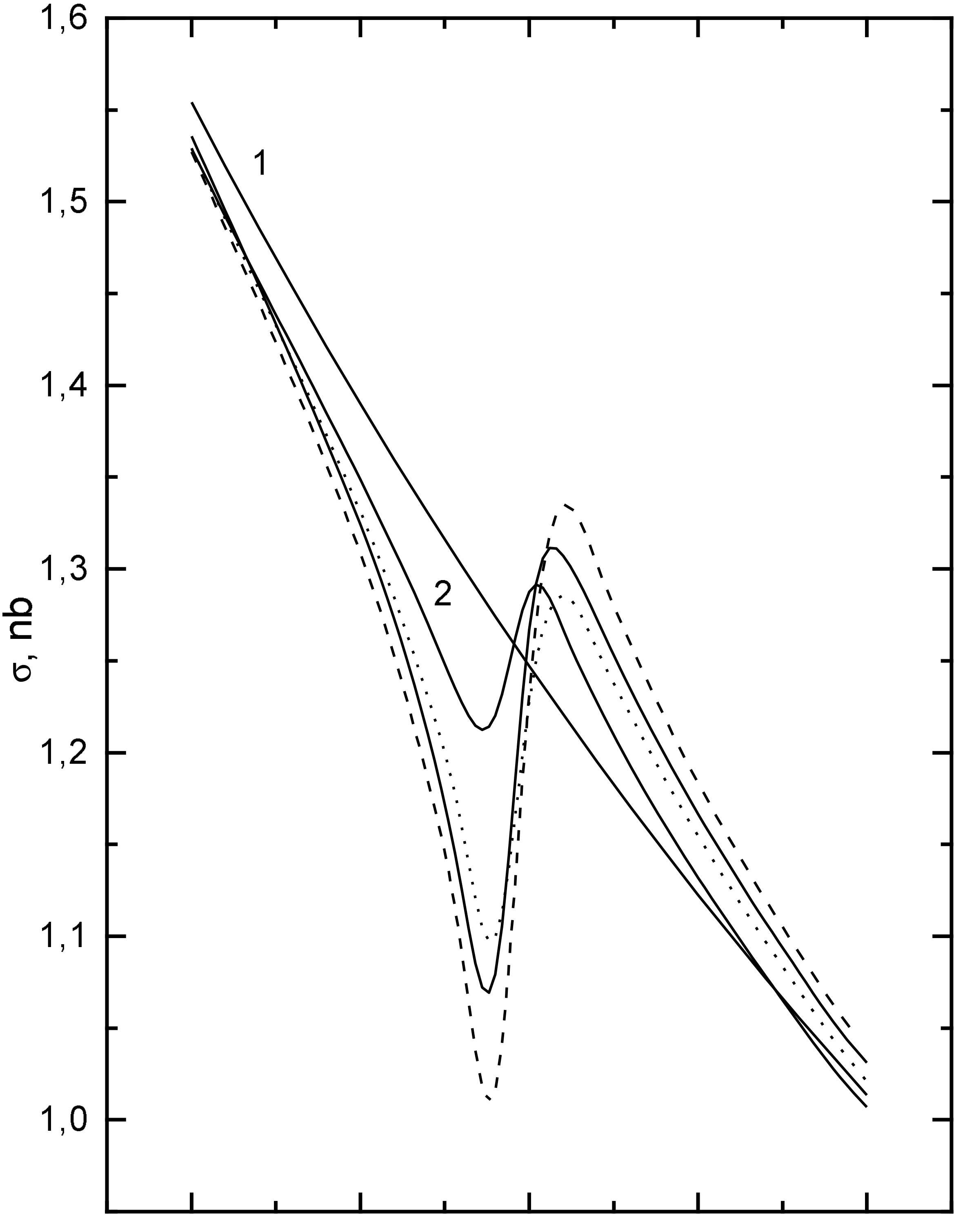

Fig. 6

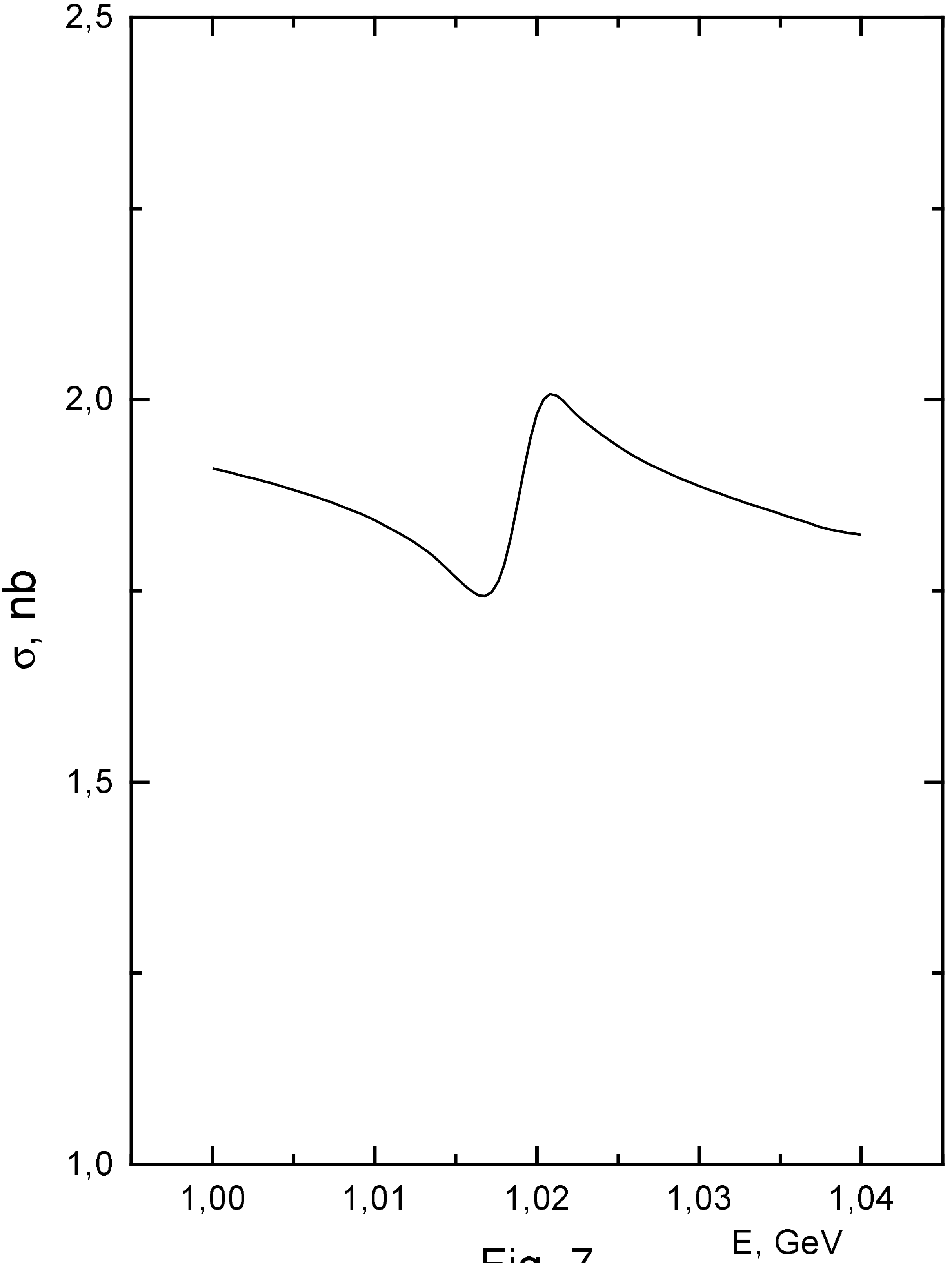

Fig. 7

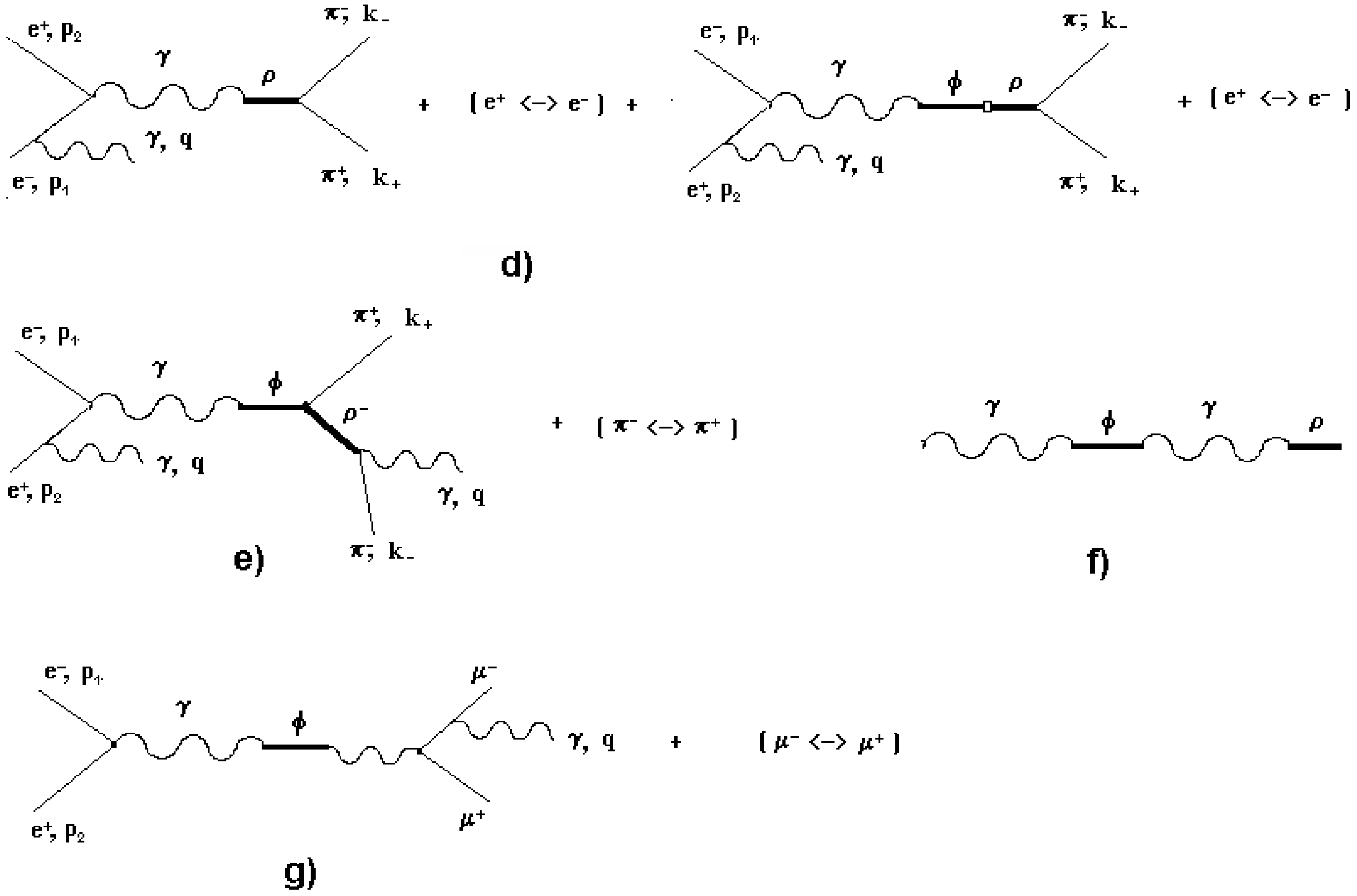
e+, p2
γ
ρ
π-, k-
π+, k+
γ, q
e-, p1
+ (e+ <-> e-) +
e-, p1
γ
φ
ρ
π-, k-
π+, k+
γ, q
e+, p2
+ (e+ <-> e-)
d)
e-, p1
γ
φ
π+, k+
ρ-
γ, q
e+, p2
γ, q
π-, k-
+ (π- <-> π+)
e)
γ
φ
γ
ρ
f)
e-, p1
γ
φ
μ-
γ, q
+ (μ- <-> μ+)
e+, p2
μ+
g)

Fig. 1